posits roughly follows the boundary of two adjacent big blocks, being substantially located along the trajectory A_{-9} of the northeast set. Similarly, several ore deposits of New Mexico and of southeastern Arizona seem to be emplaced along A_{-12} trajectory of the northeast set and the B_3 trajectory of the northwest set, that is, along two of the trajectories bounding another big block at its southern side. The corner, where the above B_3 and A_{-12} trajectories intersect, does not, unlike the preceding ones, represent an intersection of four trajectories, but only two.

The regularities as described above generally fit well in nearly the whole area of the western United States, with the exception of the westernmost part (mainly California).

Preliminary comparison of the prospecting net with the Bouger anomaly map of the United States (*11*) shows a relation in each set of trajectories. Considering the north-south set, trajectories +6 and +9 show the most pronounced relation to the gravity anomaly pattern. This relation of ore deposits to the system of four sets of empirical shear stress trajectories applies to hydrothermal deposits of various ages. The deep faults to which the trajectories are believed to correspond served interruptedly as supply channels in the metallogenetic history of this large region.

Structural control of ore deposition in the Cordilleran part of the United States has been the subject of study for many years [compare especially Butler (*12*) and other papers of the "Lindgren Volume," and many papers in the recent "Graton-Sales Volume" edited by Ridge (*13*)]. The unequal distribution of hydrothermal ore deposits of the western United States was underlined, for example, by Billingsley and Locke (*14*), who dealt with structure of the individual ore districts. Mayo (*15*) recognized the role of four systems of faults and their intersections on the localization of several bodies of igneous rocks and ore deposits in the area. Badgley (*16*) recognized that the deposits of Bingham, Park City, Tintic, and Cripple Creek lie close to the landward projection of the Mendocino zone. A relation of the Bingham District to the prolongation of the Mendocino zone was also suggested by Wisser (*17*). Landwehr (*10*) defined seven northeast-trending belts of major mineralization in this area and expressed the opinion that these belts reflect zones of deep rupture in the earth's crust.

Structural patterns of some ore districts or of larger areas of the western United States, as expressed by some authors, show a promising relation to the net of shear stress trajectories of Fig. 3. An example is the structural pattern of the southwestern copper region given by Badgley [see Fig. 5 in (*18*)].

In the central United States Heyl (*19*) recognized that economically promising sulfide deposits occur along a west-trending fault system crossing Kentucky and Missouri near the 38th parallel, particularly at associated cryptoexplosion structures along it and at the intersection of the fault system with the Cincinnati arch. Thus, it seems that the importance of the east-west shear stress trajectories for prospecting need not be limited only to the area of the western United States.

JAN KUTINA
Department of Geological Sciences,
Lehigh University,
Bethlehem, Pennsylvania 18015

References and Notes

1. J. Kutina, J. Pokorný, M. Veselá, *Econ. Geol.* **62**, 390 (1967); correction, *ibid.*, p. 1010.
2. J. Kutina, in *Endogenous Ore Deposits* (Proceedings of Section 7, 23rd International Geological Congress, Prague, 1968), pp. 99–110.
3. J. Kutina and A. Telupil, *Vestn. Ústredniho Ústavu Geol.* **41**, 431 (1966).
4. A. C. McLean and S. Johnstone, personal communication.
5. H. W. Menard, *Bull. Geol. Soc. Amer.* **66**, 1149 (1955).
6. W. N. Gilliland, *Science* **137**, 685 (1962).
7. M. D. Fuller, *Geophysics* **29**, 602 (1964).
8. H. W. Menard, *Marine Geology of the Pacific* (McGraw-Hill, New York, 1964).
9. G. V. Cohee *et al.*, *Tectonic Map of the United States, 1 : 2,500.000* (U.S. Geological Survey and American Association of Petroleum Geologists, Washington, D.C., 1962).
10. W. R. Landwehr, *Econ. Geol.* **62**, 494 (1967).
11. G. P. Woolard and H. R. Joesting, Eds., *Bouger Gravity Anomaly Map of the United States, 1 : 2,500.000* (American Geophysical Union and U.S. Geological Survey, Washington, D.C., 1964).
12. B. S. Butler, in *Ore Deposits of the Western States* (Lindgren Volume), J. W. Finch *et al.*, Eds. (American Institute of Mining, Metallurgical, and Petroleum Engineers, New York, 1933), pp. 198–326.
13. J. D. Ridge, Ed., *Ore Deposits of the United States, 1933—1967* (Graton-Sales Volume) (American Institute of Mining, Metallurgical, and Petroleum Engineers, New York, 1968), vols. 1 and 2.
14. P. Billingsley and A. Locke, *Trans. AIME* **144**, 9 (1941).
15. E. B. Mayo, *Mining Engng.* **10**, pt. 3, 1169 (1958).
16. P. C. Badgley, "Tectonic analysis as an exploration tool," *Soc. Mining Eng., AIME*, preprint 59, 169 [from S. F. Kelly, *Western Miner and Oil Rev.* (Oct. 1960)].
17. E. H. Wisser, *Can. Mining Metal. Bull.* **52**, 34 (1959).
18. P. C. Badgley, *Trans. AIME* **223**, 381 (1962).
19. A. V. Heyl, *Econ. Geol.* **63**, 585 (1968).
20. P. Laffitte and P. Rouveyrol, *Carte Minière du Globe sur Fond Tectonique au 20,000,000^e* (Bureau de Recherches Geologiques et Minière, Paris, 1964).
21. W. Burnham, "Metallogenic Provinces of the Southwestern United States and Northern Mexico" (New Mexico Institute of Mining and Technology, Socorro, Bulletin 65, 1959), pp. 1–76.
22. P. B. King, "Tectonic features," *Tectonic Map of the United States in the Scale 1 : 7,500.000* (U.S. Geological Survey, Washington, D.C., 1967).
23. I thank Dr. J. D. Ryan, chairman of the Department of Geological Sciences, for the support he has given me while I was elaborating this report during my stay at Lehigh University. Dr. Gunnar Kullerud, Geophysical Laboratory, Washington, D.C., offered valuable suggestions that improved the report. I also thank my colleagues in the Department of Geological Sciences for recommending some of the literature references, and I am especially grateful to Charles B. While for constructive discussions.

27 March 1969

■

Hydrocalcite ($CaCO_3 \cdot H_2O$) and Nesquehonite ($MgCO_3 \cdot 3H_2O$) in Carbonate Scales

Abstract. *Hydrocalcite ($CaCO_3 \cdot H_2O$) with exactly one molecule of hydrate water is the main component of carbonate scales deposited from cold water in contact with air. When the magnesium content of the water is high, the hydrocalcite occurs together with $MgCO_3 \cdot 3H_2O$ (nesquehonite). From the conditions under which hydrocalcite is transformed into calcite and aragonite, it appears that in some cases aragonite in nature may be formed by way of an intermediary of $CaCO_3 \cdot H_2O$.*

Synthesis of $CaCO_3 \cdot H_2O$ has been accomplished by precipitation at ±0°C or in the presence of additives such as polyphosphates, $MgCl_2$, and sugar (*1*, *2*). It has hitherto not been observed in nature. The compound $MgCO_3 \cdot 3H_2O$, which has been synthesized (*3*), also occurs as the mineral nesquehonite. Both hydrocarbonates are unstable.

It was thus surprising to find that $CaCO_3 \cdot H_2O$ (hereafter called hydrocalcite) is the main component of carbonate scales (i) in air scrubbers of different air-conditioning plants, and (ii) at the mouths of cold water pipes.

Table 1. Mineralogical composition of scale samples Nos. 1 through 3, as determined by x-ray analysis.

Component	Formula	Sample No. (percentage of composition) 1	2	3
Hydrocalcite	$CaCO_3 \cdot H_2O$	90	47	
Nesquehonite	$MgCO_3 \cdot 3H_2O$		38	
Calcite	$CaCO_3$	1	5	1
Aragonite	$CaCO_3$	4		95
Noncarbonates		4	10	4

If the water has a high magnesium content, $MgCO_3 \cdot 3H_2O$ is also formed.

In the air scrubbers hydrocarbonate scales are deposited only along the walls of the chambers, the reflecting panels, and in the nozzles of the water spray zone, that is, above the water surface (Fig. 1). Carbonate coatings, formed below the water surface and thus always covered by water, consist entirely of calcite. (These calcite scales have not been considered in evaluating the samples.) The carbonate crusts are 0.1 to 2 mm thick, depending on the hardness of the circulating water and the intervals at which the plants are cleaned. The temperature in such chambers is 10° to 14°C.

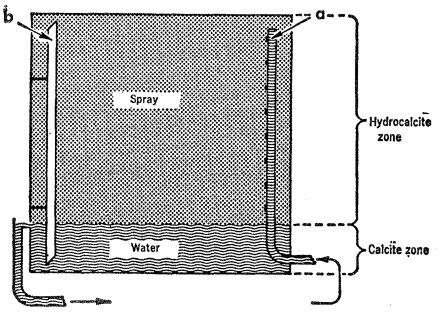

Fig. 1. Schematic section showing the air scrubber of an air-conditioning plant. (*a*) Water nozzle; (*b*) reflecting panel.

Table 2. Chemical composition of scale samples Nos. 1 and 2 and of the water from which they originate. Sample No. 3 (Table 1) has not been analyzed chemically.

Component	Sample 1 Scale* (% by weight)	Sample 1 Water (mg/liter)	Sample 2 Scale* (% by weight)	Sample 2 Water (mg/liter)
Ca	32.8	203	18.1	99
Mg	0.1	38	6.6	152
Na	1.5	55	0.9	50
Fe	0.1	< 0.01	0.04	< 0.01
CO_3	48.6		43.4	
SO_4	Tr.	207	Tr.	147
PO_4	0.05	0.15	Tr.	0.05
H_2O	13.7		21.9	
Insolubles	2.2		10.0	
Total	99.25		100.94	

* Tr. indicates trace.

The mineralogical composition of three scale samples is presented in Table 1. Table 2 shows the chemical composition of these samples and of the water from which they originate. The maximum content of hydrocalcite in the samples is 90 percent; minor components are calcite, aragonite, and noncarbonate substances (sample 1). When the data on the chemical analyses of hydrocalcite samples are reduced to a value free of anhydrous carbonate, they indicate the theoretical water content of 1 mole of H_2O per formula weight of hydrocalcite. Nesquehonite and hydrocalcite are the main components of the scales (sample 2) formed in an air scrubber of which the circulating water has an extremely high magnesium content. Older samples or samples taken from disconnected air-conditioning plants consist almost entirely of aragonite (sample 3). The low operating temperature of the chambers and the results of laboratory tests indicate that hydrocalcite is transformed into aragonite.

The hydrocarbonates were identified by x-ray diffraction (CuKα). The x-ray pattern of $MgCO_3 \cdot 3H_2O$ is only slightly different from that of synthetic nesquehonite (*4*). The x-ray diagram of $CaCO_3 \cdot H_2O$ is essentially the same as that reported by Brooks *et al.* (*1*) for synthetic $CaCO_3 \cdot H_2O$, but it is more complete. The reindexing of the powder diagram of hydrocalcite (Table 3) is based on a hexagonal recalculated unit cell with $a_0 = 6.092$ Å, $c_0 = 7.534$ Å.

Various data on the conditions and rates of transformation of synthetic $CaCO_3 \cdot H_2O$ have been reported (*1, 5*). Examination of the sample material revealed that, in same cases, carbonate crusts had formed on water taps over a period of about 1 year, and that these remained almost entirely hydrocalcite; in other cases, these crusts were dehydrated over a period of several weeks under conditions not corresponding to those of their formation.

In order to obtain more exact data, crushed samples consisting of 90 percent hydrocalcite were transformed into $CaCO_3$ in the laboratory. Heating in a dry atmosphere caused hydrocalcite to be transformed into calcite only. At 100°C the transformation period amounts to about 18 days; at 150°C the transformation period amounts to about 100 minutes.

In the presence of H_2O and regardless of whether additive ions are present or not, hydrocalcite is transformed into aragonite only; this transformation is independent of the temperature from $-2°$ to $+50°C$. One exception was found: when the water contains only HN_3, the hydrocalcite is transformed into calcite. The time required for the transformation of a room-temperature sample of $CaCO_3 \cdot H_2O$ covered by double-distilled water into aragonite is 9 days. The rate of dehydration is proportional to the temperature, but below $+12°C$ the hydrocalcite becomes stable.

Table 3. X-ray powder data of $CaCO_3 \cdot H_2O$ found in scales.

d (Å)	I/I_1	*hkl**
5.261	35	100
4.313	100	101
3.064	70	102
2.820	50	111
2.510	4	003
2.487	23	201
2.366	27	112
2.268	6	103
2.159	45	202
1.993	17	210
1.937	3	113
1.928	65	211
1.8185	9	203
1.7730	12	104
1.7624	13	212
1.7596	1	300
1.7125	1	301
1.6024	1	114
1.5935	5	302
1.5620	4	213
1.5233	4	220
1.4927	5	221
1.4495	3	105
1.4367	10	311
1.4120	1	222
1.3695	4	214
1.3642	3	312
1.3192	3	400
1.3089	2	205
1.3002	2	401

* Indexed by B. Nuber.

Certain additives (NaCl, NH_3, $FeCl_2$) in the water covering the hydrocalcite favor the transformation process, and other additives (Na_2SO_4, $SrCl_2$, $FeSO_4$, NH_4NO_3, $MgCl_2$, $BaCl_2$, sugar, polyphosphates) impede it. An increase in the concentration of these additives causes a corresponding acceleration or deceleration of the transformation in all samples investigated. Observations over a period of 3 months revealed that the presence of either < 0.1 mole percent $MgCl_2$, < 0.01 mole percent $BaCl_2$, or < 100 parts per million of Calgon in the covering water entirely prevents the transformation of $CaCO_3 \cdot H_2O$. Air-dried hydrocalcite kept in a dry place over a period of 3 months also remained unchanged. No vaterite or any other hydrate of $CaCO_3$ formed in any of the transformation experiments.

These results suggest that nesquehonite forms in scales under conditions similar to those in nature. Analogously, it may be assumed that hydrocalcite also forms in nature by precipitation from cold water in its contact zone with air, as in the spray zone of waterfalls, in nearshore parts of a lake, and in stalactites and stalagmites. Hydrocalcite is less likely to form from water rich in NaCl (seawater).

Transformation of $CaCO_3 \cdot H_2O$ into calcite takes place only as a result of dry heating; transformation into aragonite takes place only in the presence of H_2O (the exception being water rich in NH_3). Thus complete transformation into aragonite takes place even at temperatures below 0°C and in the presence of additives such as NaCl, despite the fact that in the direct crystallization of anhydrous $CaCO_3$ from solution low temperatures and the presence of NaCl favor the formation of calcite and suppress the formation of aragonite. It may thus be assumed that aragonite, whose origin in nature and in technical plants cannot be explained by the temperature and the ion content of the precipitating medium, does not form directly; rather it forms by way of a carbonate hydrate phase.

HANNELORE MARSCHNER*
Laboratorium für Sedimentforschung,
University of Heidelberg,
Heidelberg, Germany

References and Notes

1. R. Brooks, L. M. Clark, E. F. Thurston, *Phil. Trans. Roy. Soc. London Ser. A* **243**, 145 (1951).
2. G. Baron and M. Pesneau, *Compt. Rend.* **243**, 1217 (1956); R. van Tassel, *Z. Anorg. Chem.* **319**, 107 (1962).
3. H. Menzel, A. Brückner, H. Schulz, *Z. Elektrochem.* **36**, 188 (1930); M. R. Kinsolving, C. MacGillavry, R. Pepinsky, *Amer. Mineral.* **35**, 127 (1950).
4. American Society for Testing and Materials Powder Diffraction File Card No. 1-0130 (1960).
5. F. Krauss and W. Schriever, *Z. Anorg. Chem.* **188**, 259 (1930).
6. I thank A. Fritz for supplying samples, M. Gastner for chemical analyses, B. Nuber for calculating the crystallographic data, and Dr. G. Müller for many stimulating discussions. Supported by the Deutsche Forschungsgemeinschaft.

* Present address: National Building Research Institute, P.O. Box 395, Pretoria, South Africa.

20 March 1969; revised 17 June 1969 ■

Strength-Density Relations in Particulate Silicates of Complex Shape and Their Possible Lunar Significance

Abstract. *Some terrestrial particulate silicate rocks with complex particle shapes have internal friction angles over 45° and cohesion of about 0.1 newton per square centimeter at bulk densities of 0.6 to 0.8 gram per cubic centimeter. Mechanical and other properties of the lunar surface layer, observed with spacecraft, may be consistent with a low bulk density and complex reentrant shapes for the fine particles.*

Earth-based measurements of the photometry and infrared emission of the lunar surface long ago suggested that the surface is covered with fine particles with very low packing density and complex, highly irregular particle shapes. Subsequent radio emission and radar measurements seemed consistent with this hypothesis.

The Surveyor landings confirmed the presence of the fine particle cover. However, the larger surface blocks, over 1 mm in diameter, were shown in Luna and Surveyor pictures to have generally convex surfaces and to look rather solid. Furthermore, the density of one block was measured as 2.8 ± 0.4 g/cm^3, an indication that it is solid or nearly solid (*1*). As a consequence, in recent discussions of the structure and properties of the fine matrix material it has generally been assumed that the fine particles, too, have convex, rounded, surfaces and are essentially solid. On this assumption, bulk densities have been calculated for the surface layer from the mechanical properties determined with the Surveyor spacecraft (*1, 2*). The results are not in good agreement with some earth-based data and with the Luna 13 measurement of bulk density (*3*).

This discrepancy raises the possibility that the shapes and perhaps the internal porosity of the fine particles, predominantly 2 to 60 μm in diameter (*4*), which constitute the bulk of the surface layer, are different from those of the larger blocks. Consideration of the size-frequency distribution of the larger pieces and its extrapolation downward has already led to some doubt as to whether the fine and coarse fractions can be considered to come from the same population (*5*). It thus seemed worthwhile to examine further the mechanical property-density relations for silicates composed of particles with highly irregular reentrant shapes. Measurements of shear strength for such material have been reported (*6*), but data on cohesion and internal friction are desirable for comparison with lunar observations.

Volcanic ash and lapilli deposited by the 1959 activity of Kilauea Iki in Hawaii were used as an experimental material; the site of the sample was approximately 1 km southwest of the crater (*7*). The particles are essentially tholeiitic basaltic glass, with a solid density of about 2.8 g/cm^3. Figure 1 shows typical particle shapes, and Table 1 gives the particle size distribution. The material is much coarser than the fine lunar matrix but is of interest because

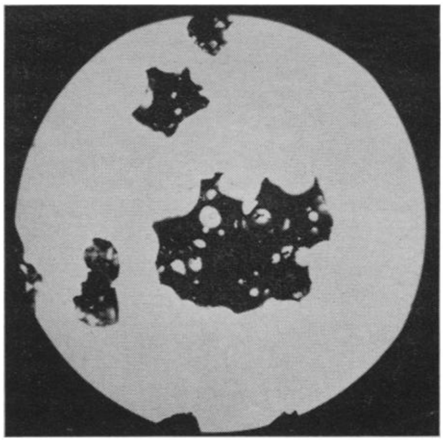

Fig. 1. Micrograph of ash particles. Diameter of the field is 2.2 mm. [Courtesy of J. Green]